Veterinary Microbiology 253 (2021) 108969

Contents lists available at ScienceDirect

Veterinary Microbiology

journal homepage: www.elsevier.com/locate/vetmic

Rescue of Senecavirus A to uncover mutation profiles of its progenies during 80 serial passages *in vitro*

Fuxiao Liu [a,*,1], Yilan Huang [a,1], Qianqian Wang [a], Juan Li [b], Hu Shan [a,*]

[a] College of Veterinary Medicine, Qingdao Agricultural University, Qingdao, 266109, China
[b] Key Laboratory of Etiology and Epidemiology of Emerging Infectious Diseases in Universities of Shandong, Shandong First Medical University & Shandong Academy of Medical Sciences, Tai'an, 271000, China

ARTICLE INFO

Keywords:
Senecavirus A
Passaging
Next-generation sequencing
SNVs
Quasispecies
Mutations

ABSTRACT

Senecavirus A (SVA), also known as Seneca Valley virus, belongs to the genus *Senecavirus* in the family *Picornaviridae*. In this study, a China SVA isolate (CH-LX-01-2016) was rescued from its cDNA clone, and then identified by RT-PCR, indirect immunofluorescence assay and mass spectrometry. The rescued SVA could separately induce typical plaque formations and cytopathic effects in cell monolayers. In order to uncover its evolutionary dynamics, the SVA was subjected to eighty serial passages *in vitro*. Its progenies per ten passages were analyzed by next-generation sequencing (NGS). The NGS analyses showed that neither sequence-deleting nor -inserting phenotype was detectable in eight progenies, within which a total of forty-one intra-host single-nucleotide variations (SNVs) arose with passaging. Almost all SNVs were identified as the single-nucleotide polymorphism with mixture of two nucleotides. SNVs led to eighteen nonsynonymous mutations, out of which sixteen could directly reflect their own frequencies of amino acid mutation, due to only one SNV occurring in their individual codons. Compared with its parental virus without passaging, the passage-80 SVA progeny had formed a viral quasispecies, as evidenced by a total of twenty-eight SNVs identified in it.

1. Introduction

Senecavirus A (SVA), also known as Seneca Valley virus, is classified into the genus *Senecavirus* in the family *Picornaviridae*. This virus can cause vesicular disease in pigs. Typical clinical signs are vesicular and/or ulcerative lesions on pigs' snout, oral mucosa, coronary bands and hooves, indistinguishable from those of other vesicular diseases, such as foot-and-mouth disease and swine vesicular disease (Liu et al., 2020b; Zhang et al., 2018). Some herds additionally suffer an increase in neonatal losses of 1- to 4-day-old piglets (Houston et al., 2020). SVA now is the only member in the genus *Senecavirus*. Its genome is a positive-sense, single-stranded and nonsegmented RNA, approximately 7300 nucleotides (nt) in length, with a 3' poly (A) tail but without a 5' capped structure. The genome contains 5' and 3' untranslated regions (UTRs), and a single long open reading frame (ORF) of polyprotein precursor. Referring to other picornaviruses (Sun et al., 2016), a polyprotein precursor of SVA can be stepwisely cleaved into twelve polypeptides, namely the L, VP4, VP2, VP3, VP1, 2A, 2B, 2C, 3A, 3B, 3C (or $3C^{pro}$) and 3D (or $3D^{pol}$).

The $3D^{pol}$ is an RNA-dependent RNA polymerase (RdRp), by which the SVA genome is replicated *via* a negative-sense RNA intermediate (Ferrer-Orta et al., 2015). The picornaviral RdRp generally lacks proofreading ability, therefore causing relatively high mutation rates during viral replication (Cameron et al., 2016; Lescar and Canard, 2009; Peersen, 2017). Mutation events would gradually accumulate to form a viral quasispecies during serial passages. Viral quasispecies is regarded as the mutant distributions (also termed mutant swarms, clouds or spectra) that are generated upon replication of RNA viruses in infected cells or hosts (Andino and Domingo, 2015).

Conventional Sanger sequencing is not capable of generating a large dataset to identify each mutation sites in viral genome at a given passage (Wu et al., 2016). Next-generation sequencing (NGS) as an alternative method has been successfully applied to analyze and to quantify the exceptionally-high diversity within viral quasispecies. Obtaining high-accuracy NGS data to uncover a viral quasispecies not only relies on error corrections of NGS data, but also depends on the well-tailored design of experimental and computational analysis approaches (Lu et al., 2020). By means of the NGS, a large number of RNA virus genomes

* Corresponding authors.
E-mail addresses: laudawn@126.com (F. Liu), shanhu67@163.com (H. Shan).
[1] The contribution is equal to this work.

https://doi.org/10.1016/j.vetmic.2020.108969
Received 5 September 2020; Accepted 20 December 2020
Available online 28 December 2020

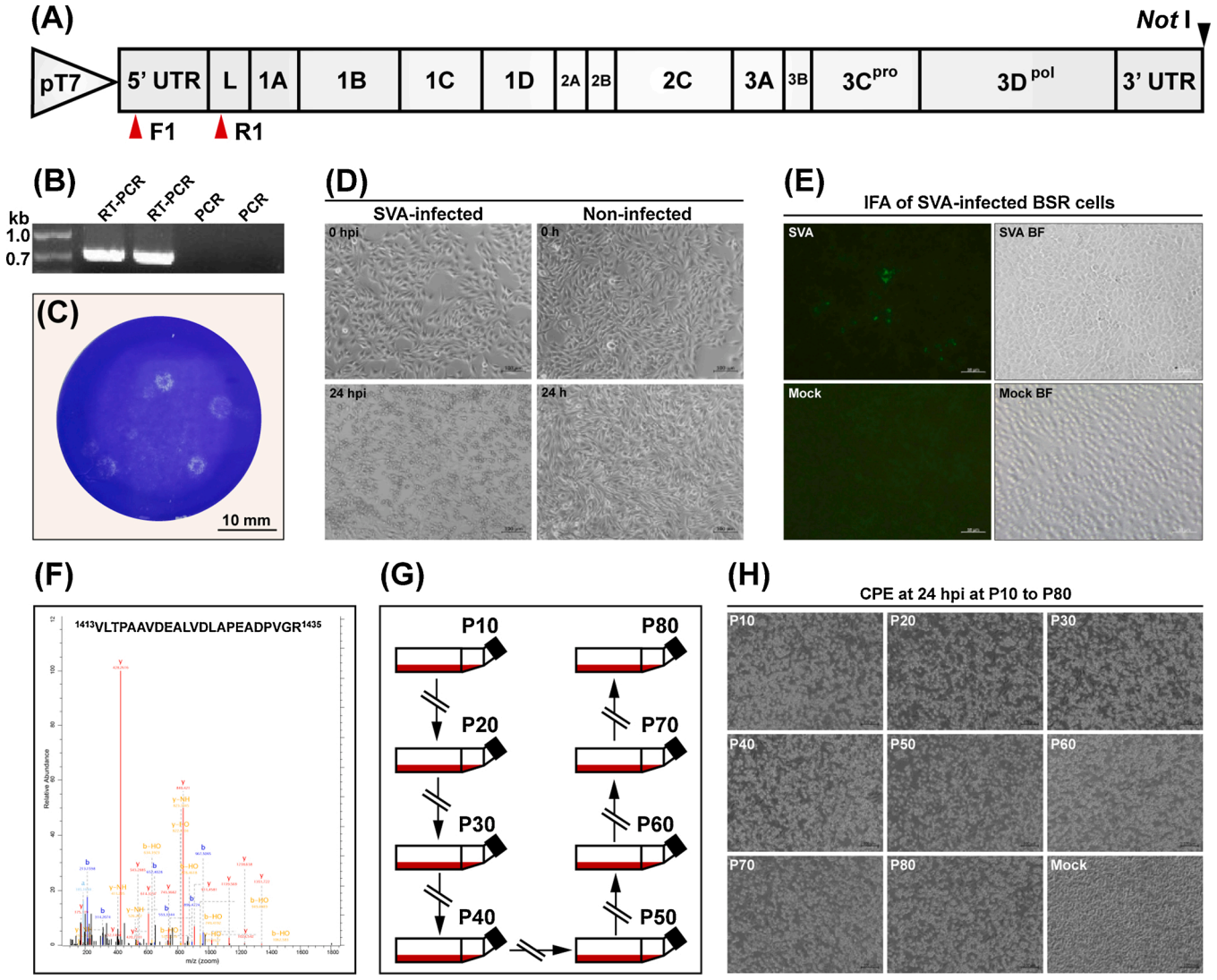

Fig. 1. Rescue, identification, characterization and passaging of SVA. Schematic representation of SVA cDNA clone (A). The F1/R1 primer-targeted sites are marked with two red arrowheads, and the *Not* I recognition site is marked with one black arrowhead. RT-PCR and PCR analyses of the P5 SVA using the F1/R1 primer pair (B). SVA-induced plaque formations on a BSR cell monolayer (C). P6 SVA- and non-infected BSR cell monolayers at 24 hpi (D). Indirect immunofluorescence assay of SVA-infected BSR cells (E). Mock: non-infected cells. One of SVA-specific MS/MS spectra on peptide identification of the P5 SVA (F). Strategy for eighty serial passages of SVA (G). CPEs induced by SVA at 24 hpi during eighty serial passages (H) (For interpretation of the references to colour in this figure legend, the reader is referred to the web version of this article).

have been sequenced and now are publicly available. More importantly, intra-host single-nucleotide variations (SNVs) in various viruses have been systematically analyzed by the NGS for uncovering their evolutionary dynamics (Campo et al., 2014; Hasing et al., 2016; Ni et al., 2016; Yang et al., 2018).

The SVA CH-LX-01-2016 was a China isolate (Zhao et al., 2017), whose reverse genetics system was developed previously. Using this system, we have rescued two recombinant SVAs, which can independently express an enhanced green fluorescent protein (eGFP) (Liu et al., 2020a) and a NanoLuc® luciferase (NLuc) (Liu et al., 2020c). In this study, the SVA CH-LX-01-2016 was rescued from its cDNA clone without genetic modification, and then subjected to eighty serial passages *in vitro* for NGS to reveal its evolutionary dynamics.

2. Materials and methods

2.1. Cell line and plasmid

The T7 RNA polymerase-expressing BHK (BSR in this study) cells were cultured at 37 °C with 5 % CO_2 in Dulbecco's modified Eagle's medium (DMEM), supplemented with 10 % fetal bovine serum (FBS) and G418 (500 μg/mL). The pcDNA™3.1(+) plasmid (Thermo Fisher, Waltham, MA, USA) was used for constructing the SVA CH-LX-01-2016 (GenBank: KX751945.1) cDNA clone.

2.2. Construction of SVA cDNA clone

The SVA cDNA clone was flanked by the T7 promoter and the *Not* I sequences at its 5′ and 3′ ends, respectively (Fig. 1A). The 5′- and 3′-end-modifying cDNA clone was chemically synthesized and subcloned into the pcDNA™3.1(+) plasmid. The recombinant plasmid was purified using a HighPure Maxi Plasmid Kit (TIANGEN, Beijing, China) according to the manufacturer's instruction.

2.3. Rescue of SVA

The SVA cDNA clone was linearized by digestion with *Not* I restriction endonuclease (Takara, Dalian, China), followed by agarose gel electrophoresis for extraction of the linearized plasmid from gel by a gel extraction kit (TIANGEN, Beijing, China). The purified cDNA clone was used for transfection of BSR cells to rescue SVA (Passage-0, P0) using Lipofectamine 2000 (Thermo Fisher, Waltham, MA, USA) according to the manufacturer's instruction. The cDNA clone-transfected cells were harvested at 72 h post transfection (hpt), and subjected to one freeze-and-thaw cycle to collect supernatant for serial blind passages in BSR cells.

2.4. RT-PCR analysis

The P5 SVA was harvested for extracting viral RNA by a Viral RNA/DNA Extraction Kit (Takara, Dalian, China) according to the manufacturer's instruction. The extracted RNA was used as template for RT-PCR analysis using a High Fidelity One Step RT-PCR Kit (Takara, Dalian, China). The forward (F1: 5′-AGGCACAGAGGAGCAACATCCAA-3′) and reverse (R1: 5′-ATCGTTCACCGATCTAGGGTATT-3′) primers were designed for amplifying a 693-bp fragment. The RT-PCR reaction underwent 45 °C for 10 min, 94 °C for 2 min and then 30 cycles at 98 °C (10 s), 55 °C (15 s) and 68 °C (10 s). The extracted RNA was simultaneously subjected to PCR analysis using the F1/R1 primers. The PCR reaction contained 2 × PrimeSTAR Max Premix (Takara, Dalian, China) and underwent 30 cycles at 98 °C (10 s), 55 °C (5 s) and 72 °C (10 s). RT-PCR and PCR products were detected by agarose gel electrophoresis, followed by Sanger sequencing for analyzing the RT-PCR product.

2.5. Plaque assay

Serial 10-fold dilutions were made by mixing 120 μL of SVA with 1080 μL of DMEM. One mL of each dilution was seeded to individual wells of a 6-well plate containing confluent BSR cells. The plate was incubated at 37 °C for 1.5 h before the layer of 1% low melting point agarose (in DMEM with 10 % FBS) was added. The cell monolayers were fixed in 4% paraformaldehyde at 72 hpi, and then stained with 0.2 % crystal violet. Plaque morphology was observed after washing the plate with tap water.

2.6. Indirect immunofluorescence assay

BSR cells were infected (MOI = 1) with the P5 SVA for 12 h, and then fixed with 4% paraformaldehyde for 30 min. After fixation, cells were washed four times with PBS, and then permeated with 0.4 % Triton X-100 for 30 min. After permeation, cells were washed three times with PBS and blocked in blocking solution at 37 °C for 1 h. Subsequently, cells were incubated with the anti-VP1 monoclonal antibody at 37 °C for 2 h, washed three times with PBS, and incubated with the Alexa Fluor® 488 conjugate (Thermo Fisher, Waltham, MA, USA) at 37 °C for 1 h. Cells were washed three times with PBS, coated with 90 % glycerin, and visualized under the fluorescence microscope.

2.7. Mass spectrometry

The P5 SVA in culture supernatant was inactivated by 0.1 % formalin at 4 °C for 48 h, and subsequently subjected to mass spectrometry (MS) at the Shanghai Bioprofile Biotechnology Co., Ltd (Shanghai, China). Briefly, protein digestion was performed with a method of filter-aided sample preparation, as described previously (Wiśniewski et al., 2009). Liquid chromatography linked to tandem mass spectrometry (LC–MS/MS) was performed on a Q Exactive Plus mass spectrometer that was coupled to Easy nLC (Thermo Fisher, Waltham, MA, USA). The MS data were analyzed using MaxQuant software v1.6.0.16. The database search results were filtered and exported with <1 % false discovery rate at peptide-spectrum-matched level, and protein level, respectively.

2.8. Serial passages of SVA for NGS

The rescued SVA was serially passaged in BSR cells for eighty passages (Fig. 1G), approximately 24 h/passage. The culture supernatants of SVA at the P10, P20, P30, P40, P50, P60, P70 and P80 were independently harvested for extracting viral RNA as described in Subheading 2.4. A total of eight RNA samples were separately reverse transcribed using the 1st Strand cDNA Synthesis Kit (Takara, Dalian, China) and random hexamers, according to the manufacturer's instruction. The Illumina sequencing and library construction were performed at the Shanghai Tanpu Biotechnology Co., Ltd (Shanghai, China). In brief, the NEBNext® Ultra™ II RNA Library Prep Kit (NEB, Ipswich, MA, USA) was used for library construction. After adapter ligation, ten cycles of PCR amplification were performed for sequencing target enrichment. The libraries were pooled at equal molar ratio, denatured and diluted to optimal concentration prior to sequencing. The Illumina NovaSeq 6000 (Illumina, San Diego, CA, USA) was used for sequencing to generate pair-end 150 bp reads.

2.9. Processing and analysis of NGS data

Raw reads were filtered by fastp (https://github.com/OpenGene/fastp) to remove sequencing adapters and low-quality reads, including those reads scored < Q20. Ribosomal RNAs and host reads subtraction by read-mapping were performed with BBMap program (https://github.com/BioInfoTools/BBMap). *De novo* genome assembly was performed using SPAdes v3.14.1 (https://github.com/ablab/spades), as described previously (Nurk et al., 2013). These

Table 1
SVA-specific peptide sequences matching to tandem mass spectrometry (MS/MS) spectra.

Matching peptide sequences
^{57}SFNEYQIR^{64}
^{130}GGLAGLLTNFSGILNPLGYLKDHNTEEMENSADR^{163}
^{400}EGATTDPEITFSVR^{413}
^{484}IPTLMAFGR^{492}
^{972}MVHSVQQTWR^{981}
^{1116}ASPVLQYQLEMK^{1127}
^{1182}QTSAQRVEPVVVVLRGK^{1198}
^{1312}INYDLTLEVSEAYK^{1325}
^{1413}VLTPAAVDEALVDLAPEADPVGR^{1435}
^{1482}APRSENAYDGPKK^{1494}
^{1750}PEFEPAVLSKFDPR^{1763}
^{1885}PSEKVR^{1890}
^{2033}TALALTYK^{2040}

extracted assembled scaffolds limited the minimum contig length to 100 bases, with the best BLAST hits to the NCBI nucleotide database.

High-quality filtered reads were mapped against the SVA reference genome (GenBank: KX751945.1) by Burrows-Wheeler Aligner v0.7.17 (http://bio-bwa.sourceforge.net/), which also generated BAM file to calculate the mapping depth and coverage. Single-nucleotide polymorphisms (SNPs) were identified using an integrated software package, Snippy v4.4.5 (https://github.com/tseemann/snippy), which included both substitutions and insertions/deletions. The available SNP results were selected if mapping quality was ≥ 60 and depth was ≥10.

3. Results

3.1. SVA was rescued from its cDNA clone

The SVA cDNA clone was schematically shown in Fig. 1A. The *Not* I-linearized cDNA clone was purified to transfect BSR cells for rescuing the P0 SVA. The cDNA-transfected cell culture was subjected to one freeze-and-thaw cycle at 72 hpt, and the supernatant was collected for serial blind passages. SVA-induced cytopathic effects (CPEs) were invisible until the third blind passage.

3.2. RT-PCR confirmed recovery of SVA

Total RNA of the P5 virus was analyzed by the F1/R1-based RT-PCR. The F1/R1 primer-targeted sites were shown in Fig. 1A. One product was loaded into two sample wells. Expected bands of 693-bp amplicon appeared only on the RT-PCR lanes (Fig. 1B, Lane RT-PCR). The PCR control (Fig. 1B, Lane PCR) indicated no cDNA residues affecting the RT-PCR analysis. The Sanger sequencing revealed the RT-PCR product identical to the 693-bp sequence.

3.3. SVA induced plaque formation and cytopathic effect

SVA-induced plaque morphology was determined by the plaque assay. Plaque formations were morphologically intact on the BSR cell monolayer at 72 hpi (Fig. 1C). The plaque diameter ranged 3–4 mm. The P6 SVA could induce typical CPEs on the BSR cell monolayer at 24 hpi

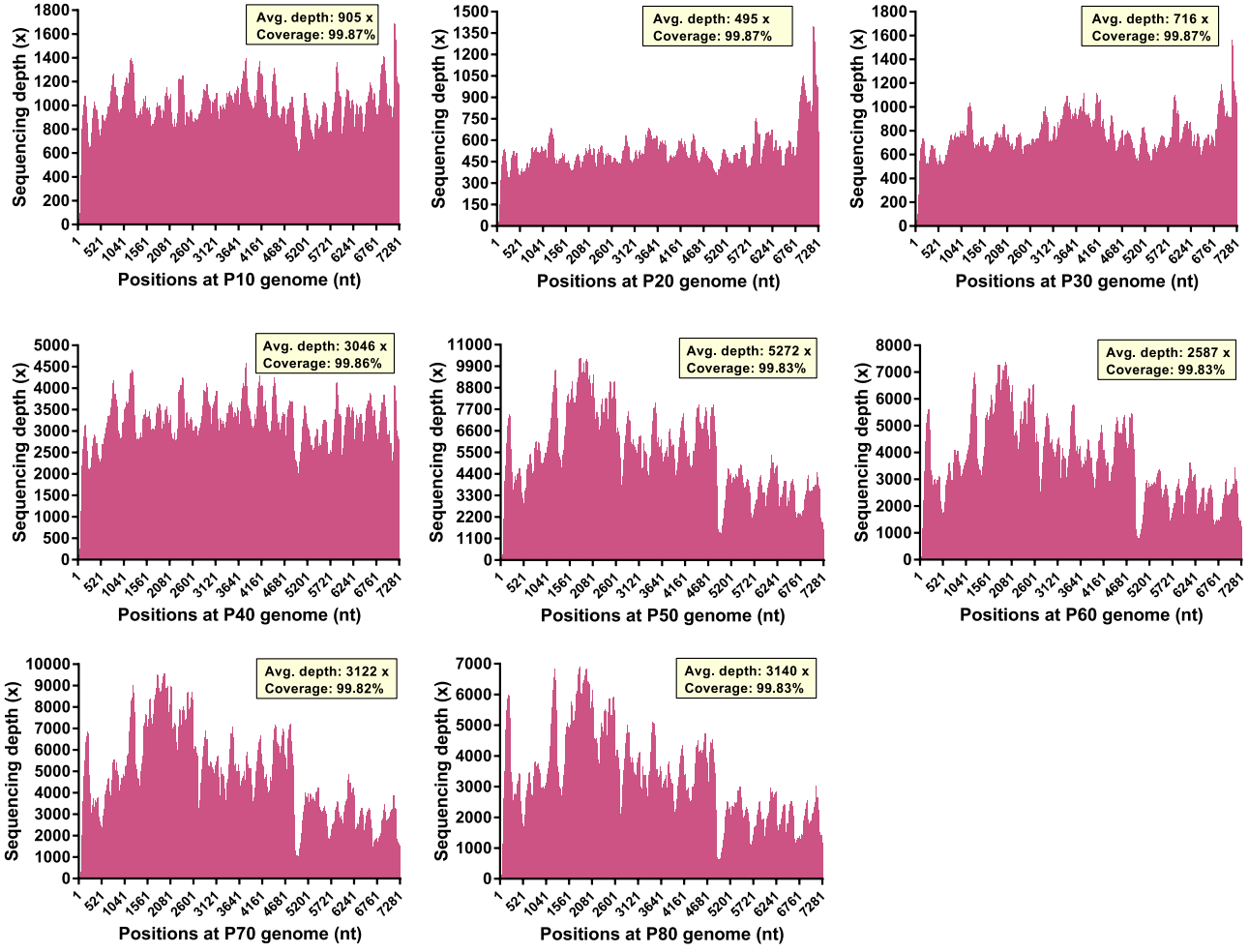

Fig. 2. Depth and coverage of next-generation sequencing for each SVA sample at different passage. The P20 and P50 show the lowest (495×) and highest (5272×) average sequencing depths, respectively.

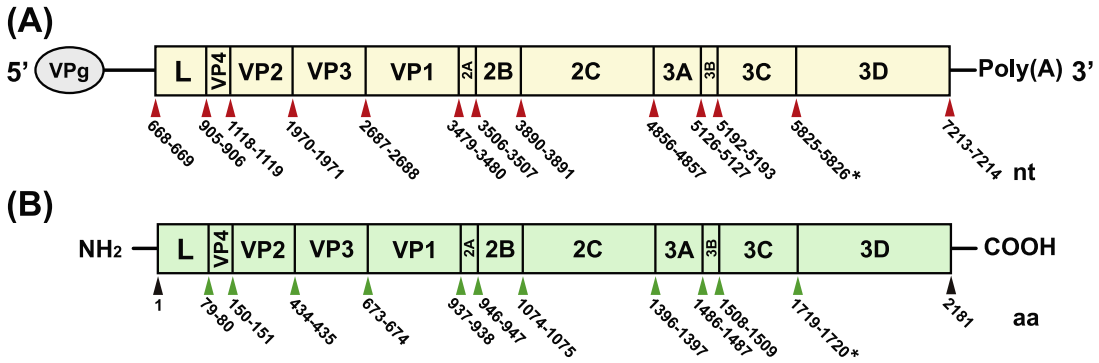

Fig. 3. Schematic representations of SVA CH-LX-01-2016 genome and polyprotein. Each red arrowhead illustrates a site either between two adjacent genes or between a UTR and a gene (A). *Either of potential sites (Hales et al., 2008). Each green arrowhead illustrates a site between two adjacent proteins. Two black arrowheads separately mark the first and the last amino acids in the polyprotein (B). *Either of potential sites (Hales et al., 2008) (For interpretation of the references to colour in this figure legend, the reader is referred to the web version of this article).

(Fig. 1D), such as cell rounding, lysis and detachment from flask.

3.4. IFA and MS showed VP1 and polyprotein expressions, respectively

The IFA was performed for assessing VP1 expression of the P5 SVA using anti-VP1 monoclonal antibody and Alexa Fluor® 488 conjugate. Green fluorescence was visible on the SVA- but not non-infected cell monolayer (Fig. 1E), demonstrating the VP1 expression in cells. Polyprotein expression by the P5 SVA was confirmed further by MS. A total of thirteen SVA-specific peptide sequences matched to the MS/MS spectra (Table 1), out of which one representative was shown in Fig. 1F.

3.5. NGS yielded analyzable sequencing depth and coverage

SVA-induced robust CPEs, like cell rounding, lysis and detachment (Fig. 1H), could appear as early as 24 hpi, or even earlier, during eighty serial passages (Fig. 1G). Eight (P10, P20, P30, P40, P50, P60, P70 and P80) total RNA samples were extracted for the NGS, yielding analyzable sequencing depth and coverage (Fig. 2 and Supplementary Table 1). Their average depths were 905, 495, 716, 3046, 5272, 2587, 3122 and 3140×, respectively. All eight samples remained a high (>99.8 %) coverage range across the full reference sequence (GenBank: KX751945.1). Uncovered and low-depth regions were only located at the 5′- and 3′-end regions of the SVA genome.

3.6. Forty-one SNVs arose with 80 serial passages

The full-length sequence of SVA CH-LX-01-2016 genome was schematically illustrated in Fig. 3A. The NGS analyses showed that neither sequence-deleting nor -inserting phenotype was detectable in eight progenies, within which a total of forty-one SNVs arose with passaging. Fig. 4A and B showed absolute and relative sequencing depths for all SNVs at each passage, respectively. All SNV profiles with serial passages were shown in Fig. 5. Except three-nucleotide coexistence at nt 5494 (P40) and nt 7284 (P50), almost all SNVs were identified as a SNP with mixture of two nucleotides. All SNVs could be classified into seven main types (Table 2), described as follows.

The 5′ and 3′ UTRs separately exhibited two SNVs: T133C (5′ UTR), A58T (5′ UTR), A7283G (3′ UTR) and A7284G (3′ UTR), out of which the last three were identified with low-depth NGS data. Other SNVs were located in the single long ORF of polyprotein precursor. Some SNV sites, such as C1363T, C1670T and G3297A, appeared at a given passage, would be maintained for dozens of passages, but finally reverted back to their original statuses with viral passaging. In contrast, nt 734, 1435 and 1954 gradually underwent the single-nucleotide substitution from an earlier passage to P80, and consequently three original nucleotides, "G" (nt 734), "A" (nt 1435) and "G" (nt 1954), were almost totally replaced with "A", "G" and "A" at P80, respectively. Four site mutations arose as early as P10, whereas many others, *e.g.*, T3317C and T3741G, did not appear until P80. There were a few low-frequency point mutations, like A1727C and G2494C, occurring once only at a single passage. Four major sites, nt 4900, 4948, 5493 and 5796, gradually revealed SNPs with relatively equal nucleotide compositions with passaging.

3.7. SNVs caused 18 single amino acid mutations

The full-length amino acid (aa) sequence of SVA CH-LX-01-2016 was schematically illustrated in Fig. 3B. Thirty-seven SNVs in SVA polyprotein ORF led to eighteen amino acid positions with nonsynonymous mutation, out of which sixteen directly showed their own mutation frequencies, due to only one SNV occurring in their individual codons (Fig. 6). The other two mutation positions, aa 1411 (Fig. 6, G1411?) and 1609 (Fig. 6, D1609?), owing to separately harboring two SNVs (Fig. 6, 4899 nt$^{@}$-4900 nt$^{@}$ and 5493 nt$^{@}$-5494 nt$^{@}$), possibly showed a phenotype characterized by coexistence of multiple amino acid mutations. For example, two adjacent SNVs (G4899A-G4900C) might cause the coexistence of three mutated amino acids (G1411A, G1411S and G1411T) at aa 1411. Except aa 1411 and 1609, other sixteen positions independently showed identical mutation frequencies to those of their SNVs. Out of twelve SVA polypeptides, the L, VP2, VP3, VP1, 2B, 2C, 3A and 3C separately showed at least one nonsynonymous mutation; the VP4 and 3D simply showed silent mutations; the 2A and 3B had neither nonsynonymous nor silent mutation.

4. Discussion

SVA was an emerging virus that recently affected numerous pig farms in China (Qian et al., 2016; Sun et al., 2018; Wang et al., 2017; Zhu et al., 2017). The SVA CH-LX-01-2016 was a China isolate (Zhao et al., 2017), whose reverse genetics system was developed in this study. Using this system, we had previously rescued two reporter-tagged recombinant SVAs (Liu et al., 2020a, c). Recovery of the competent SVA from its cDNA clone was identified by RT-PCR and IFA. The former showed a typical positive result (Fig. 1B), whereas the latter only exhibited weak fluorescence emitting from the SVA-infected cell monolayer (Fig. 1E). In order to confirm the expression of SVA polyprotein, the inactivated P5 SVA was analyzed by the MS, which showed a total of thirteen SVA-specific peptide sequences that matched to the MS/MS spectra (Table 1). The purified P6 virion or, less probably, procapsid (Strauss et al., 2018), revealed a sphere-like shape under our observation by transmission electron microscopy (Liu et al., 2020b), but not shown in the present study. SVA-induced robust CPEs could even appear as early as 24 hpi after the rescued SVA underwent five serial passages, indicating that it adapted gradually to consecutive passages *in*

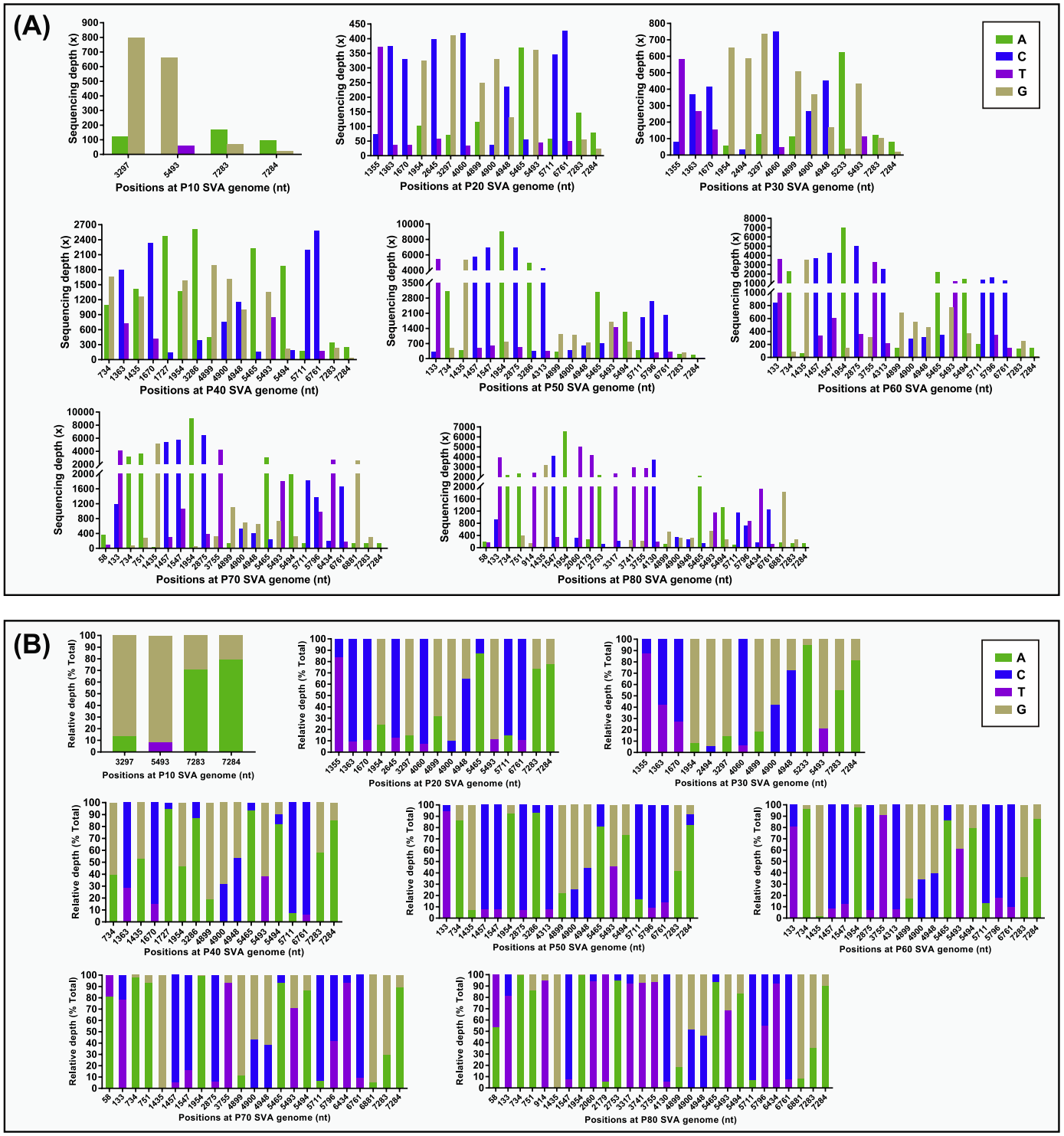

Fig. 4. Absolute (A) and relative (B) depths of next-generation sequencing for detectable positions with single-nucleotide polymorphism at each passage.

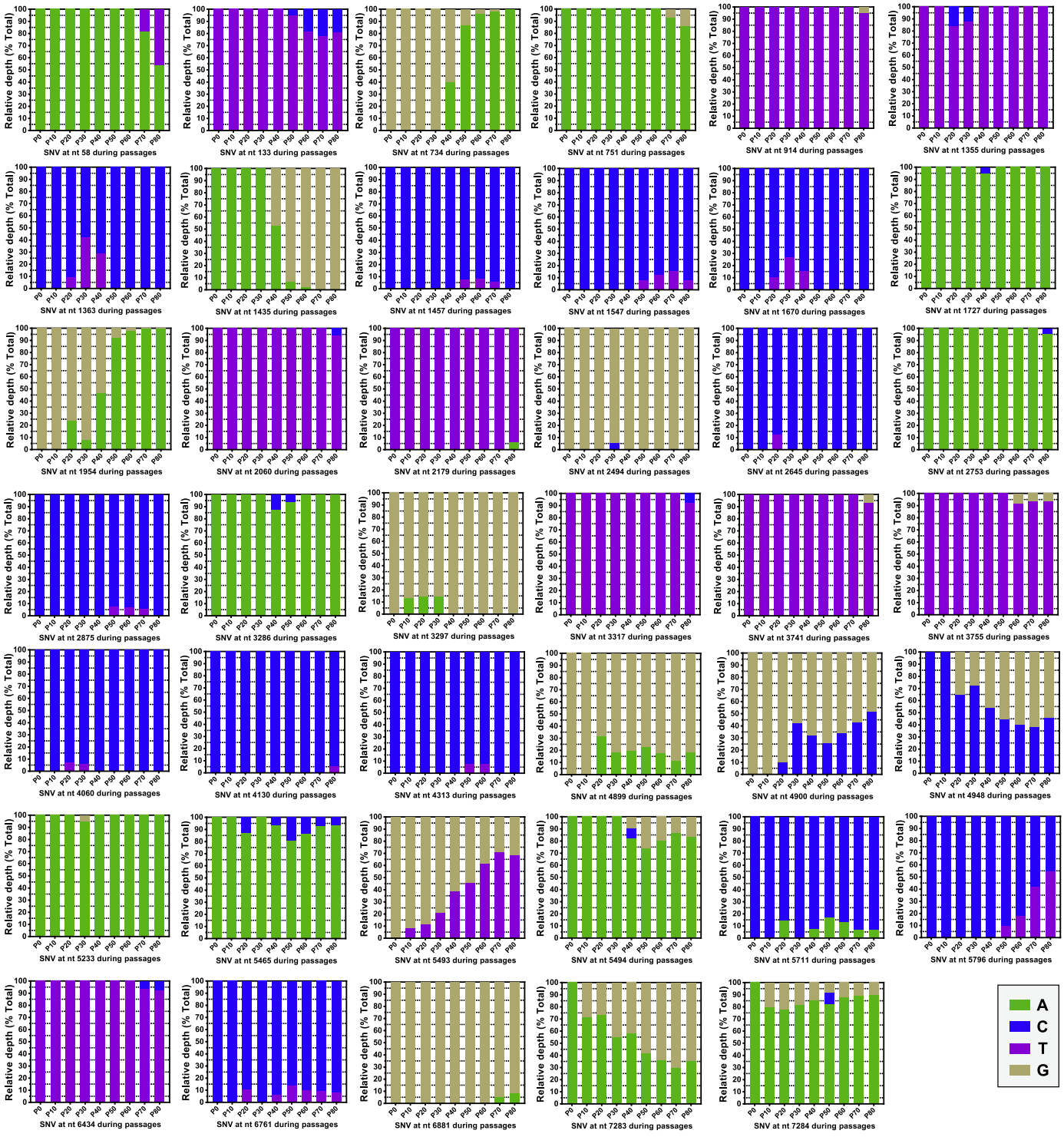

Fig. 5. Relative depths of next-generation sequencing for forty-one single nucleotide variations in SVA with eighty serial passages.

Table 2
Seven types of single nucleotide variations in SVA genome during viral passaging.

Types	Characteristics	Representatives	Passages
I	Relatively low sequencing depth	A58T	P70 and P80
		A7283G	P10 to P80
		A7284G	P10 to P80
II	Reverting back to original status	C1363T	P20 to P40
		C1670T	P20 to P40
		G3297A	P10 to P30
III	Almost totally replaced at P80	G734A	P40 to P80
		A1435G	P40 to P80
		G1954A	P20 to P80
IV	Appearing as early as P10	G3297A	P10 to P30
		G5493T	P10 to P80
V	Unidentified until P80	T3317C	P80
		T3741G	P80
VI	Low-frequency and occurring once	A1727C	P40
		G2494C	P30
VII	Relatively equal nucleotide compositions	G4900C	P70 and P80
		C4948G	P40 to P80

vitro.

Most RNA viruses are genetically unstable during replication, owing to the low fidelity properties of their RdRps (Coffey et al., 2011; Jin et al., 2011; Sierra et al., 2000; Steinhauer et al., 1992; Ward et al., 1988). Error-prone replication is a major factor to generate RNA viruses' quasispecies in their progenies. An accurate estimate of mutation events is crucial to understand the evolutionary mechanism of a given RNA virus. Although conventional Sanger sequencing is still the gold standard for determining viral mutations, its time- and labor-consuming operations with limited sensitivity greatly reduce its applicability to large-scale studies of viral quasispecies. The NGS as an alternative method, capable of generating a large dataset to identify each mutation sites in viral genomes, hence has been used for analyzing and quantifying the exceptionally-high diversity of viral quasispecies (Huang et al., 2019; Lu et al., 2020).

In this study, in order to analyze its quasispecies diversity, the rescued SVA was serially passaged in BSR cells for eighty passages. The reason why we used one rescued SVA, rather than another isolate, was that the former, recovered from its cDNA clone, contained no any mutations at P0. Nevertheless, any of isolates is not characterized by such a genotype at P0, regardless of whether it has been purified. Point mutations are theoretically restricted only in a few sites during the first several passages. Indeed, we found only four SNVs at P10, whereas the P20 showed twelve additional ones in viral genome, implying that the P20 progeny had begun to form viral quasispecies. Out of all forty-one SNVs, the G5493T was a unique one that always existed as an SNP phenotype during P10 and P80. The nt 5493 gradually underwent nucleotide substitution with serial passaging (Fig. 5). Its adjacent position, nt 5494, also exhibited an SNP status since P40 (Fig. 5), at which, interestingly, three nucleotides (A, C and G) coexisted. Because nt 5493, 5494 and 5495 jointly formed a codon, the G5493T and A5494G/C possibly led to the coexistence of five mutated amino acids (G, A, Y, C and S) at a single position at P40. However, the mutation frequency could not be determined for each mutant.

It has been widely confirmed that the low fidelity of RdRp leads to high mutation rates in RNA viruses (Andino and Domingo, 2015; Borderia et al., 2016). Li et al. (2019) recently demonstrated that a single amino acid mutation (S460L) in SVA (HLJ/CHA/2016) $3D^{pol}$ could significantly enhance the fidelity of RdRp (Li et al., 2019). In the present study, we used the CH-LX-01-2016 sequence as a backbone to rescue the wild-type SVA. The position 460 in its $3D^{pol}$ is a leucine in itself, and therefore the SVA in this study is theoretically a high-fidelity strain, according to the conclusion of Li et al. (2019) (Li et al., 2019). In our other studies, we also used the CH-LX-01-2016 sequence as a backbone to construct two reporter-tagged recombinant SVAs, rSVA-eGFP (Liu et al., 2020a) and rSVA-NLuc (Liu et al., 2020c). Both recombinants, albeit theoretically characterized by high-fidelity replication *in vitro*, were prone to losing their foreign sequences. We found that the rSVA-eGFP was more likely to do so than the rSVA-NLuc, possibly attributed to a longer non-self sequence in the former. Unfortunately, we did not rescue another recombinant SVA with modification of L460S in the $3D^{pol}$ for comparing its genetic fidelity with that of wild-type SVA, rSVA-eGFP or rSVA-NLuc.

Sometimes we found that typical clinical signs could not be

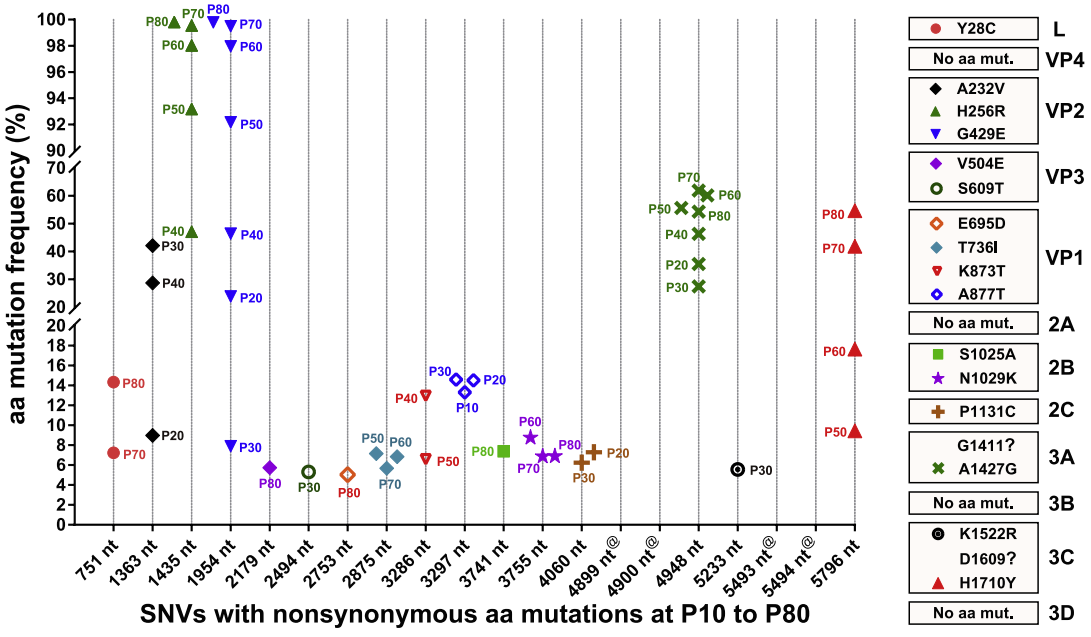

Fig. 6. Frequencies of nonsynonymous amino acid mutations caused by single nucleotide variations in SVA with serial passages. The "4899 nt@-4900 nt@" and "5493 nt@-5494 nt@" imply the possible coexistence of multiple amino acid mutations at aa 1411 and 1609, respectively.? : Possible coexistence of multiple amino acid mutations; Mut.: Mutation.

reproduced after experimental infection with some SVA strains that had even been isolated from diseased pigs. Therefore, the CH-LX-01-2016 strain, albeit isolated from a diseased pig, was not necessarily a high-virulence strain. Although a challenge experiment was not performed in pigs for determining the virulence of rescued SVA CH-LX-01-2016, we found that neither Balb/c nor Kunming mice showed clinical signs after intramuscular, subcutaneous or intraperitoneal injection with the P5 SVA (data not shown). Quasispecies diversity of RNA viruses has been demonstrated to affect possibly the pathogenic potential of a given viral population (Ciota et al., 2007; Jerzak et al., 2007; Korboukh et al., 2014; Markussen et al., 2013; Meng et al., 2015). In general, viral virulence in animals can be progressively attenuated with virus consecutive passages *in vitro* (Liu et al., 2016). Thus, the P80 SVA was most probably a virulence-attenuated strain, irrespective of its original virulence at the first several passages.

Declaration of Competing Interest

The authors report no declarations of interest.

Acknowledgements

This work was supported by the National Key R&D Program for the 13th Five-Year Plan, China (2016YFD050110404) and the Shandong Key Research and Development Program, China (2019GNC106074). We gratefully thank Tao Hu and Xue Yao, Shandong First Medical University & Shandong Academy of Medical Sciences, for their help in analyzing our NGS data. We also thank the China Animal Health and Epidemiology Center for offering the BSR cell line to us.

Appendix A. Supplementary data

Supplementary material related to this article can be found, in the online version, at doi:https://doi.org/10.1016/j.vetmic.2020.108969.

References

Andino, R., Domingo, E., 2015. Viral quasispecies. Virology 479–480, 46–51.
Borderia, A.V., Rozen-Gagnon, K., Vignuzzi, M., 2016. Fidelity variants and RNA quasispecies. Curr. Top. Microbiol. Immunol. 392, 303–322.
Cameron, C.E., Moustafa, I.M., Arnold, J.J., 2016. Fidelity of nucleotide incorporation by the RNA-dependent RNA polymerase from poliovirus. Enzymes 39, 293–323.
Campo, D.S., Dimitrova, Z., Yamasaki, L., Skums, P., Lau, D.T., Vaughan, G., Forbi, J.C., Teo, C.G., Khudyakov, Y., 2014. Next-generation sequencing reveals large connected networks of intra-host HCV variants. BMC Genomics 15 (Suppl. 5), S4.
Ciota, A.T., Ngo, K.A., Lovelace, A.O., Payne, A.F., Zhou, Y., Shi, P.Y., Kramer, L.D., 2007. Role of the mutant spectrum in adaptation and replication of West Nile virus. J. Gen. Virol. 88, 865–874.
Coffey, L.L., Beeharry, Y., Borderia, A.V., Blanc, H., Vignuzzi, M., 2011. Arbovirus high fidelity variant loses fitness in mosquitoes and mice. Proc. Natl. Acad. Sci. U. S. A. 108, 16038–16043.
Ferrer-Orta, C., Ferrero, D., Verdaguer, N., 2015. RNA-dependent RNA polymerases of picornaviruses: from the structure to regulatory mechanisms. Viruses 7, 4438–4460.
Hales, L.M., Knowles, N.J., Reddy, P.S., Xu, L., Hay, C., Hallenbeck, P.L., 2008. Complete genome sequence analysis of Seneca Valley virus-001, a novel oncolytic picornavirus. J. Gen. Virol. 89, 1265–1275.
Hasing, M.E., Hazes, B., Lee, B.E., Preiksaitis, J.K., Pang, X.L., 2016. A next generation sequencing-based method to study the intra-host genetic diversity of norovirus in patients with acute and chronic infection. BMC Genomics 17, 480.
Houston, E., Temeeyasen, G., Piñeyro, P.E., 2020. Comprehensive review on immunopathogenesis, diagnostic and epidemiology of Senecavirus A. Virus Res. 286, 198038.
Huang, S.W., Hung, S.J., Wang, J.R., 2019. Application of deep sequencing methods for inferring viral population diversity. J. Virol. Methods 266, 95–102.
Jerzak, G.V., Bernard, K., Kramer, L.D., Shi, P.Y., Ebel, G.D., 2007. The West Nile virus mutant spectrum is host-dependent and a determinant of mortality in mice. Virology 360, 469–476.
Jin, Z., Deval, J., Johnson, K.A., Swinney, D.C., 2011. Characterization of the elongation complex of dengue virus RNA polymerase: assembly, kinetics of nucleotide incorporation, and fidelity. J. Biol. Chem. 286, 2067–2077.
Korboukh, V.K., Lee, C.A., Acevedo, A., Vignuzzi, M., Xiao, Y., Arnold, J.J., Hemperly, S., Graci, J.D., August, A., Andino, R., Cameron, C.E., 2014. RNA virus population diversity, an optimum for maximal fitness and virulence. J. Biol. Chem. 289, 29531–29544.
Lescar, J., Canard, B., 2009. RNA-dependent RNA polymerases from flaviviruses and Picornaviridae. Curr. Opin. Struct. Biol. 19, 759–767.
Li, C., Wang, H., Shi, J., Yang, D., Zhou, G., Chang, J., Cameron, C.E., Woodman, A., Yu, L., 2019. Senecavirus-specific recombination assays reveal the intimate link between polymerase fidelity and RNA recombination. J. Virol. 93, e00576–00519.
Liu, F., Wu, X., Li, L., Zou, Y., Liu, S., Wang, Z., 2016. Evolutionary characteristics of morbilliviruses during serial passages *in vitro*: gradual attenuation of virus virulence. Comp. Immunol. Microbiol. Infect. Dis. 47, 7–18.
Liu, F., Huang, Y., Wang, Q., Shan, H., 2020a. Construction of eGFP-tagged senecavirus a for facilitating virus neutralization test and antiviral assay. Viruses 12, E283.
Liu, F., Wang, Q., Huang, Y., Wang, N., Shan, H., 2020b. A 5-year review of Senecavirus A in China since its emergence in 2015. Front. Vet. Sci. 7, 567792.
Liu, F., Wang, Q., Huang, Y., Wang, N., Shan, H., 2020c. Rescue of NanoLuc luciferase-expressing Senecavirus A with oncolytic activity. Virus Res. 292, 198232.
Lu, I.N., Muller, C.P., He, F.Q., 2020. Applying next-generation sequencing to unravel the mutational landscape in viral quasispecies. Virus Res. 283, 197963.
Markussen, T., Sindre, H., Jonassen, C.M., Tengs, T., Kristoffersen, A.B., Ramsell, J., Numanovic, S., Hjortaas, M.J., Christiansen, D.H., Dale, O.B., Falk, K., 2013. Ultra-deep pyrosequencing of partial surface protein genes from infectious Salmon Anaemia virus (ISAV) suggest novel mechanisms involved in transition to virulence. PLoS One 8, e81571.
Meng, C., Qiu, X., Yu, S., Li, C., Sun, Y., Chen, Z., Liu, K., Zhang, X., Tan, L., Song, C., Liu, G., Ding, C., 2015. Evolution of newcastle disease virus quasispecies diversity and enhanced virulence after passage through chicken air sacs. J. Virol. 90, 2052–2063.
Ni, M., Chen, C., Qian, J., Xiao, H.X., Shi, W.F., Luo, Y., Wang, H.Y., Li, Z., Wu, J., Xu, P. S., Chen, S.H., Wong, G., Bi, Y., Xia, Z.P., Li, W., Lu, H.J., Ma, J., Tong, Y.G., Zeng, H., Wang, S.Q., Gao, G.F., Bo, X.C., Liu, D., 2016. Intra-host dynamics of Ebola virus during 2014. Nat. Microbiol. 1, 16151.
Nurk, S., Bankevich, A., Antipov, D., Gurevich, A.A., Korobeynikov, A., Lapidus, A., Prjibelski, A.D., Pyshkin, A., Sirotkin, A., Sirotkin, Y., Stepanauskas, R., Clingenpeel, S.R., Woyke, T., McLean, J.S., Lasken, R., Tesler, G., Alekseyev, M.A., Pevzner, P.A., 2013. Assembling single-cell genomes and mini-metagenomes from chimeric MDA products. J. Comput. Biol. 20, 714–737.
Peersen, O.B., 2017. Picornaviral polymerase structure, function, and fidelity modulation. Virus Res. 234, 4–20.
Qian, S., Fan, W., Qian, P., Chen, H., Li, X., 2016. Isolation and full-genome sequencing of Seneca Valley virus in piglets from China, 2016. Virol. J. 13, 173.
Sierra, S., Davila, M., Lowenstein, P.R., Domingo, E., 2000. Response of foot-and-mouth disease virus to increased mutagenesis: influence of viral load and fitness in loss of infectivity. J. Virol. 74, 8316–8323.
Steinhauer, D.A., Domingo, E., Holland, J.J., 1992. Lack of evidence for proofreading mechanisms associated with an RNA virus polymerase. Gene 122, 281–288.
Strauss, M., Jayawardena, N., Sun, E., Easingwood, R.A., Burga, L.N., Bostina, M., 2018. Cryo-electron microscopy structure of Seneca Valley virus procapsid. J. Virol. 92, e01927–01917.
Sun, D., Chen, S., Cheng, A., Wang, M., 2016. Roles of the picornaviral 3C proteinase in the viral life cycle and host cells. Viruses 8, 82.
Sun, Y., Cheng, J., Wu, R.T., Wu, Z.X., Chen, J.W., Luo, Y., Xie, Q.M., Ma, J.Y., 2018. Phylogenetic and genome analysis of 17 novel Senecavirus A isolates in Guangdong Province, 2017. Front. Vet. Sci. 5, 314.
Wang, H., Li, C., Zhao, B., Yuan, T., Yang, D., Zhou, G., Yu, L., 2017. Complete genome sequence and phylogenetic analysis of Senecavirus A isolated in Northeast China in 2016. Arch. Virol. 162, 3173–3176.
Ward, C.D., Stokes, M.A., Flanegan, J.B., 1988. Direct measurement of the poliovirus RNA polymerase error frequency in vitro. J. Virol. 62, 558–562.
Wiśniewski, J.R., Zougman, A., Nagaraj, N., Mann, M., 2009. Universal sample preparation method for proteome analysis. Nat. Methods 6, 359–362.
Wu, X., Liu, F., Li, L., Zou, Y., Liu, S., Wang, Z., 2016. Major mutation events in structural genes of peste des petits ruminants virus through serial passages in vitro. Virus Genes 52, 422–427.
Yang, Z., Mammel, M., Whitehouse, C.A., Ngo, D., Kulka, M., 2018. Inter- and intra-host nucleotide variations in hepatitis a virus in culture and clinical samples detected by next-generation sequencing. Viruses 10, 619.
Zhang, X., Zhu, Z., Yang, F., Cao, W., Tian, H., Zhang, K., Zheng, H., Liu, X., 2018. Review of Seneca Valley virus: a call for increased surveillance and research. Front. Microbiol. 9, 940.
Zhao, X., Wu, Q., Bai, Y., Chen, G., Zhou, L., Wu, Z., Li, Y., Zhou, W., Yang, H., Ma, J., 2017. Phylogenetic and genome analysis of seven Senecavirus A isolates in China. Transbound. Emerg. Dis. 64, 2075–2082.
Zhu, Z., Yang, F., Chen, P., Liu, H., Cao, W., Zhang, K., Liu, X., Zheng, H., 2017. Emergence of novel Seneca Valley virus strains in China, 2017. Transbound. Emerg. Dis. 64, 1024–1029.